



**HAL**  
open science

# One-pot organometallic synthesis of well-controlled gold nanoparticles by gas reduction of Au(I) precursor: a spectroscopic NMR study

Pierre-Jean Debouttière, Yannick Coppel, Philippe Behra, Bruno Chaudret,  
Katia Fajerweg

## ► To cite this version:

Pierre-Jean Debouttière, Yannick Coppel, Philippe Behra, Bruno Chaudret, Katia Fajerweg. One-pot organometallic synthesis of well-controlled gold nanoparticles by gas reduction of Au(I) precursor: a spectroscopic NMR study. *Gold bulletin: a quarterly review of research on gold and its applications in industry*, 2013, 46 (4), pp.291 - 298. 10.1007/s13404-013-0117-6 . hal-02646787

**HAL Id: hal-02646787**

**<https://hal.inrae.fr/hal-02646787>**

Submitted on 29 May 2020

**HAL** is a multi-disciplinary open access archive for the deposit and dissemination of scientific research documents, whether they are published or not. The documents may come from teaching and research institutions in France or abroad, or from public or private research centers.

L'archive ouverte pluridisciplinaire **HAL**, est destinée au dépôt et à la diffusion de documents scientifiques de niveau recherche, publiés ou non, émanant des établissements d'enseignement et de recherche français ou étrangers, des laboratoires publics ou privés.

# One-pot organometallic synthesis of well-controlled gold nanoparticles by gas reduction of Au(I) precursor: a spectroscopic NMR study

Pierre-Jean Debouttière · Yannick Coppel ·  
Philippe Behra · Bruno Chaudret · Katia Fajerweg

Published online: 30 October 2013

© The Author(s) 2013. This article is published with open access at SpringerLink.com

**Abstract** A stable colloidal solution of gold nanoparticles (AuNPs) has been prepared in tetrahydrofuran by gas reduction of AuCl(tetrahydrothiophene) and alkylamines (1-octylamine, 1-dodecylamine, and 1-hexadecylamine) as stabilizing agents. Carbon monoxide is a better reducing agent than hydrogen. The important parameters for control of the synthesis of AuNPs are the temperature, the molar ratio of ligand/metal, and the structure of the stabilizing agent. A high concentration of long alkyl chains (10 eq.) favours the control of the growth of AuNPs of defined size and shape with a diameter of 4.7 nm and a narrow size distribution. For the first time, liquid-state combined with solid-state NMR

spectroscopies were used in order to determine the role of the long chain alkylamines in the synthesis of AuNPs in CO atmosphere. This combination enables the understanding of the complex chemistry of the surface of AuNPs involved in the stabilization of the AuNPs. Indeed, carbamide species were formed during the synthesis. They were strongly coordinated to the surface of AuNPs and exchange phenomena of the alkylamines present in solution occurred, too.

**Keywords** Au(I) precursor · Organometallic synthesis · Gold nanoparticles · NMR spectroscopy

**Electronic supplementary material** The online version of this article (doi:10.1007/s13404-013-0117-6) contains supplementary material, which is available to authorized users.

P.-J. Debouttière · Y. Coppel · K. Fajerweg  
CNRS, LCC (Laboratoire de Chimie de Coordination), 205 route de  
Narbonne, BP 44099, 31077 Toulouse Cedex 4, France

P.-J. Debouttière · Y. Coppel · K. Fajerweg (✉)  
UPS, INPT, Université de Toulouse, 31077 Toulouse Cedex 4,  
France  
e-mail: katia.fajerweg@lcc-toulouse.fr

B. Chaudret (✉)  
INSA, CNRS, UPS, LPCNO, Université de Toulouse,  
31077 Toulouse, France  
e-mail: bruno.chaudret@insa-toulouse.fr

P. Behra  
INPT, INRA, Université de Toulouse, UMR 1010, ENSIACET,  
4 allée Emile Monso, 31030 Toulouse CEDEX 4, France

P. Behra  
LCA (Laboratoire de Chimie Agro-industrielle), INRA,  
31030 Toulouse, France

P.-J. Debouttière  
RTRA “Sciences et Technologies pour l’Aéronautique et l’Espace”,  
31030 Toulouse, France

## Introduction

Since the 1990s, the formation of self-assembled nanostructures and the deposition of metallic nanoparticles (MNPs) have been the subject of growing interest. MNPs are now commonly used in many applications such as electronics [1, 2], catalysis [3], environmental sciences [4, 5], medicine [6, 7], and sensors [8–10]. Indeed, highly sensitive miniature sensors require advanced technology coupled with fundamental knowledge of biology, material sciences, and chemistry. Among the MNPs, gold nanoparticles (AuNPs) have been extensively studied for their optical properties [11] their absence of toxicity [12] their catalytic properties [13, 14] and their high conductivity [15–17] that make them excellent nanomaterials for various sensors such as electrochemical sensors [18, 19]. The development of simple methods to obtain AuNPs which are able to form thin films on substrates is therefore of great interest. Recently, different electrochemical methods were investigated for the deposition of AuNPs on glassy carbon electrodes for Hg(II) trace detection in water [20, 21]. Despite good performance with a detection limit of 0.40 nmol of

Hg.L<sup>-1</sup>, no control of shape and dispersity of AuNPs smaller than 15 nm were obtained by electrodeposition of HAuCl<sub>4</sub> in sodium nitrate electrolyte. As the catalysis and electrocatalysis performance depend strongly on the AuNP shape and size, it is of primary importance to control both of these parameters.

Several methods can be used to obtain well-defined AuNPs, in particular chemical reduction of molecular or ionic gold precursors. Au(III) and Au(I) are the common oxidation states of gold. Au(I), as an intermediate oxidation state, is well known to play an important role in controlling the morphology of metallic gold nanostructures synthesized from Au(III) ions [22] but only a few Au(I) precursors have been used to generate AuNPs. A recent review reports numerous advantages starting with an Au(I) precursor: (i) energy saving, (ii) easier reduction, (iii) better control of morphology, and (iv) in situ capping of nanostructures [23]. In this context, some examples of organometallic Au(I) complexes of alkylphosphines [24, 25] or (alkyl)amines [26, 27] have been reported to be efficient precursors for synthesizing gold Au<sub>55</sub> clusters or AuNPs with different shapes such as nanospheres, nanorods, nanorice [28], and nanowires [29].

In our group, we have developed a methodology for the synthesis of MNPs from organometallic precursors in organic solvents and their efficient stabilization by various ligands which allows us to get MNPs with tuneable surface properties [30]. The mild temperature and gas pressure applied for the precursor decomposition permit the synthesis of stable MNPs with a great versatility in particle size and shape. The reasons for this interest were (i) the possibility to control the kinetics of the decomposition of the precursor and therefore the size of the particles, (ii) the possibility to prepare novel structures through the mild conditions involved, and (iii) the control of surface state.

AuNPs synthesis by the decomposition of AuCl (tetrahydrothiophene) (AuCl(THT)) in an organic solvent under H<sub>2</sub> or CO in the presence of alkylamine of different alkyl chain length has led to well-defined NPs that can be self-assembled on a TEM grid [26]. However, good control of the size and stability of the particles could not be obtained through the mild decomposition of the AuCl-(alkylamine) complexes. In order to avoid the preparation and purification of AuCl-(alkylamine) complex, a one-pot synthesis in tetrahydrofuran (THF) using AuCl(THT) and alkylamines as stabilizing agent (1-octylamine(OA), 1-dodecylamine (DDA), and 1-hexadecylamine (HDA)) has been developed to control the growth of the AuNPs. In this work, we report the formation of a stable colloidal solution of AuNPs. To the best of our knowledge, this is the first time that the liquid-state NMR combined with the solid-state NMR has been used to determine the exact role of the alkylamine ligands in the synthesis of AuNPs based on the decomposition of AuCl-(alkylamine) complex under CO or H<sub>2</sub>. This original approach is very useful in the characterization of the species coordinated at the surface and also provides the formation and

the stabilization of well-controlled AuNPs <15 nm with a narrow size distribution.

## Experimental section

### Reagents and general procedures

All operations concerning nanoparticle synthesis were carried out in Schlenk tubes or Fischer–Porter glassware or in a glove box in an argon atmosphere.

OA, DDA, and HDA were purchased from Acros Organics or Sigma-Aldrich-Fluka and used without further purification.

Solvents were dried and distilled before use: THF over sodium benzophenone. All reagents and solvents were degassed before use by means of three freeze–pump–thaw cycles.

Samples for TEM analyses were prepared in the glove box by slow evaporation of a drop of crude colloidal solution deposited onto porous carbon-covered copper grids under argon. The TEM analyses were performed at the “Service Commun de Microscopie Electronique de l’Université Toulouse-III Paul Sabatier” (UPS-TEMSCAN). TEM images were obtained using a JEOL 1011 electron microscope operating at 100 kV with a resolution point of 4.5 Å. The size distributions were determined through a manual analysis of 200 NPs of enlarged micrographs with the ImageTool software to obtain a statistical size distribution and a mean diameter.

All chemical shifts for <sup>1</sup>H and <sup>13</sup>C are relative to Me<sub>4</sub>Si (TMS). 1D and 2D <sup>1</sup>H-<sup>1</sup>H correlated spectroscopy (COSY), <sup>1</sup>H-<sup>13</sup>C heteronuclear single quantum coherence (HSQC), and heteronuclear multiple bond correlation (HMBC). NMR experiments in the liquid state were recorded on a Bruker Avance 500 spectrometer equipped with a 5-mm triple resonance inverse Z-gradient probe (TBI <sup>1</sup>H, <sup>31</sup>P, BB). 2D nuclear overhauser effect spectroscopy (NOESY) measurements were done with a mixing time of 100 ms. Diffusion measurements were made using the stimulated echo pulse sequence. The recycle delay was adjusted to 3 s.

Solid-state NMR experiments were recorded on a Bruker Avance 400 spectrometer equipped with a 4-mm probe. For <sup>13</sup>C direct polarization (DPMAS) small flip angle (~30°) was used with a recycle delay of 10 s. <sup>13</sup>C cross polarization (CPMAS) spectra were recorded with a recycle delay of 5 s and contact time of 2 ms.

### Synthesis of gold nanoparticles (AuNPs)

The Au(I) precursor, AuCl(THT), was synthesized according to the procedure reported by Laguna et al., [31]. This solid is stored at -22 °C and protected from UV light in a glove box and was stable for months.

For a typical synthesis, 20 mg of AuCl(THT) (0.062 mmol) stored in a glove box was introduced into a Fisher–Porter

reactor, protected from UV light by aluminum foil and left in vacuum for 30 min. Solid amines were chosen as ligands (L: HDA or DDA with a molar ratio  $[L]/[Au]=2$  corresponding to 30 and 23 mg, respectively) and were introduced into a Schlenk tube and then left in a vacuum for 30 min. 40 mL of THF, previously degassed by three freeze–pump cycles were then added onto the amines. For octylamine (liquid at room temperature), OA was introduced onto the THF with a micropipette (20  $\mu$ L for 2 eq.).

The THF solution containing the alkylamine was transferred by a Teflon cannula into the reactor. The Fisher–Porter reactor was heated to 70 °C and then pressurized with 3 bars of H<sub>2</sub> or 1 bar of CO. The CO evacuation is done by 3 cycles of vacuum/argon. After 18 h, a homogeneous red colloidal solution was obtained and this will be referred to as “well-controlled synthesis”. This ruby-red solution was evaporated in vacuum before the addition of a solution of deoxygenated pentane (2 mL). A red/violet solution was then obtained and precipitated by the addition of 50 mL of acetone. The supernatant was eliminated by filtration. The precipitate was washed a second time with 50 mL of acetone, filtered and dried under vacuum, giving rise to the AuNPs as a dark-violet powder. TEM grids are prepared from the crude colloidal solution.

The AuNPs synthesized by the typical procedure will be denoted Au@L<sub>*i*</sub> for AuNPs obtained with *i* equivalent of the L ligand. *i* refers to the molar L/Au ratio (L or RNH<sub>2</sub>/ OA (C<sub>8</sub>H<sub>17</sub>NH<sub>2</sub>), DDA (C<sub>12</sub>H<sub>25</sub>NH<sub>2</sub>), HDA(C<sub>16</sub>H<sub>33</sub>NH<sub>2</sub>)).

## Results and discussion

### Synthesis of gold nanoparticles from the decomposition of AuCl(THT) precursor

Scheme 1 represents the one-pot synthesis of AuNPs in organic solvent with alkylamines (RNH<sub>2</sub>) as stabilizing agents using H<sub>2</sub> or CO as the reducing agent. OA, DDA, and HDA are known to be effective compounds for the stabilization of metallic nanoparticles in organic solvents [32]. In this work, neither separation nor purification of the intermediate Au(I)Cl-amine complex is needed to synthesize AuNPs in contrast with previous reports of our group [26]. Protection from the UV light was necessary as Au(I)Cl(THT) is light sensitive.

### Influence of the reducing gas in the presence of octylamine

OA was considered first because of its relatively low boiling point (ca 175 °C) compared to amines with longer alkyl chain. Thus, a homogeneous deposit on the electrode could be

expected as it would be easier to remove the excess of this ligand. The first series of experiments was performed in the presence of a small excess of OA (2, 5, 10 eq./Au). The excess of OA was not higher than 10 eq. to limit the AuNP purification step. The reduction of Au(I) precursor was first studied using H<sub>2</sub> (3 bars) either at room temperature (r.t.) or 70 °C for 18 h (overnight). In the case of 10 eq. OA, an incomplete decomposition of the Au(I) precursor was observed. Indeed, the colour of the solution was light pink/violet regardless of the reaction temperature. TEM images only show polydisperse and polymorphous AuNPs (ESM S1). This result clearly indicates that H<sub>2</sub> is not a suitable reducing agent to control the shape and the size of AuNPs in the presence of an excess of OA.

In a second set of experiments, H<sub>2</sub> was replaced by CO. After 18 h, the solution is colourless and a black precipitate is formed whatever the temperature. This indicates that CO is an effective reducing agent for the decomposition of Au(I) precursor in the presence of OA. However, OA does not seem to be able to stabilize AuNPs under these conditions as the alkyl chain is not long enough. To minimize the formation of this black precipitate, a decrease of the reaction time appears to be an alternative. A third set of experiments were carried out under the same conditions as in the second one, but with the time of exposure to CO shortened to 20 min. After 20 min under CO at r.t., the colour of the solution is ruby red. TEM images reveal polydisperse AuNPs, i.e., small (ca 2 nm) and a few tenths of nanometer AuNPs (ESM S2). It is noteworthy that these AuNPs are stable for weeks in argon but are not stable more than 2 h in air.

Moreover, it is well known that an increase of the temperature tends to give more homogenous colloidal solutions [33]. Thus, the same synthesis (10 eq OA) was run at 70 °C in CO for 20 min. After the evacuation of CO, the solution was stirred overnight in argon at 70 °C and the final solution of AuNPs is ruby red. TEM images show polydisperse AuNPs but the general overview is better than that obtained at r.t. Indeed, the majority of the AuNPs are spherical with an average size of 9 nm whereas some polymorphous AuNPs of a few tenths of nanometers are also present (ESM S3). As in the previous case, these AuNPs are stable for months both in argon and air. From these results, CO clearly appears to be the best reducing agent and will be used for the following experiments.

### Influence of the stabilizing agent

To avoid the formation of gold aggregates, primary amines with a longer alkyl chains such as DDA (C<sub>12</sub>) and HDA (C<sub>16</sub>) were



**Scheme 1** Synthesis of AuNPs by gas reduction of AuCl(THT) in the presence of alkylamine

used as ligands. The first series of experiments were performed at r.t. for 18 h (overnight) with HDA as the stabilizing agent as it has a longer alkyl chain. For a molar ratio  $[HDA]/[Au]$  of 2 or 10 eq., an intense dark-blue solution was obtained after 18 h due to the presence of polymorphous AuNPs (ESM S4). These AuNPs are stable for weeks both in argon and air.

At 70 °C, the solubility of HDA in THF is enhanced, leading to a ruby-red solution after 18 h in CO. TEM analyses (Fig. 1) of this homogeneous solution show the presence of spherical AuNPs of  $7.2 \pm 0.9$  nm when using 2 eq. of HDA. This colloidal solution is stable for months both in argon and air.

The increase of the molar ratio  $[Ligand]/[Metal]$  is expected to favour the smaller size: the same experiment was performed with a molar ratio  $[HDA]/[Au]$  of 10. A similar ruby-red solution was obtained but containing AuNPs of  $4.7 \pm 0.9$  nm (ESM S5). This experiment is a strong evidence for the role of the increase in the stabilizing agent concentration (HDA) favouring the decrease in the size of spherical AuNPs to  $4.7 \pm 0.9$  nm but has no morphological change. In order to compare the influence of the length of the amine alkyl chain, another set of experiments was performed with DDA under the same conditions with a molar ratio  $[DDA]/[Au]=2:1$  or 10:1.

The colour of the solution is again ruby red for 2 or 10 eq. of DDA. These AuNPs are stable for months under argon or air. Figure 2 shows TEM images of AuNPs obtained with 2 eq. of DDA (molar ratio of  $[DDA]/[Au]=2:1$ ).

The size of AuNPs is  $7.4 \pm 1.0$  nm and  $6.1 \pm 0.7$  nm for 2 and 10 eq. (ESM S6), respectively. The size of AuNPs is similar with 2 eq. DDA and HDA but is smaller with a molar ratio of 10 for HDA (4.7 nm vs 6.1 nm). This result indicates that a higher concentration of long alkyl chains favours the control of the growth of well-shaped and sized AuNPs.

It is noteworthy that similar AuNPs were obtained at 60 °C by Xia et al. [27] using Au(I)Cl as a precursor and oleylamine (OLA, C<sub>18</sub>) or octadecylamine (ODA, C<sub>18</sub>H<sub>37</sub>NH<sub>2</sub>) as stabilizer without any additional reducing agent. These amines have a higher steric hindrance than DDA and HDA. The

comparison between CO-assisted decomposition (our work) and thermodecomposition (Xia's work) of Au(I) precursor in the presence of amines reveals that only 2 eq. of alkylamines (DDA or HDA) are necessary to obtain AuNPs of 7.0 nm with a narrow size distribution (Figs. 1 and 2) whereas 20 eq. of OLA are needed for the synthesis of AuNPs of ca. 10 nm. In addition, the AuNPs formed in the presence of ODA showed an average size of ca. 100 nm, eight times larger than that of the AuNPs synthesized with OLA. This difference was attributed to a stronger coordination of OLA due to the presence of the olefinic C=C bond which may also coordinate to Au. In our case, the higher the concentration of HDA (or DDA), the smaller the particle size is. The AuNPs formed from the decomposition of AuCl-(NH<sub>2</sub>R) complex in CO (1 bar) at 70 °C follow a seeding growth approach. The HDA probably plays two roles, as weak reducing agent and stabilizing agent. HDA should favour the nucleation of Au(0) atoms and control the growth of the AuNPs involving the complexation in the form of Au<sub>n</sub>(0)[AuCl-HDA].

The data of the different syntheses of AuNPs obtained by the decomposition of AuCl(THT) in the THF under gas reduction in the presence of alkylamine ligands are summarized in Table S1 (ESM Table S1).

In summary, it is clearly seen that the use of DDA or HDA as stabilizing agent in THF at 70 °C in CO (1 bar) overnight leads to stable and well defined AuNPs with a narrow size distribution (<1.0 nm). NMR characterization was performed to understand the stabilization of the AuNPs.

NMR characterization of the formation of AuCl(amine) complex

The first step of the reaction between 2 eq. of amine (DDA or HDA) and the Au(I) precursor AuCl(THT) in THF at 25 °C was characterized by liquid-state NMR (ESM S7). This spectrum shows a strong evidence of the formation of AuCl-(HDA) complex (labelled # on ESM S7). Moreover,

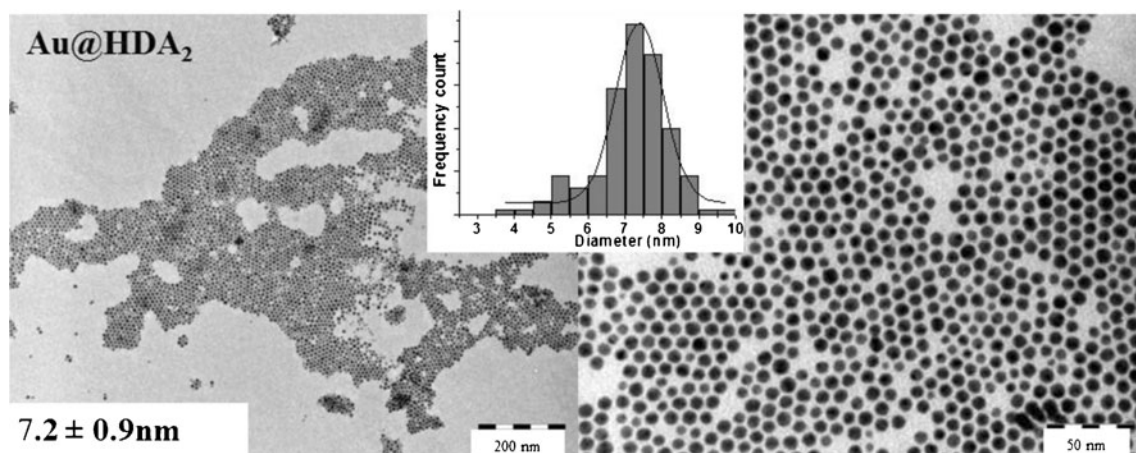


**Fig. 1** Au@HDA<sub>2</sub> obtained from the decomposition of AuCl(THT) with HDA in THF in CO overnight at 70 °C (see Table S1)

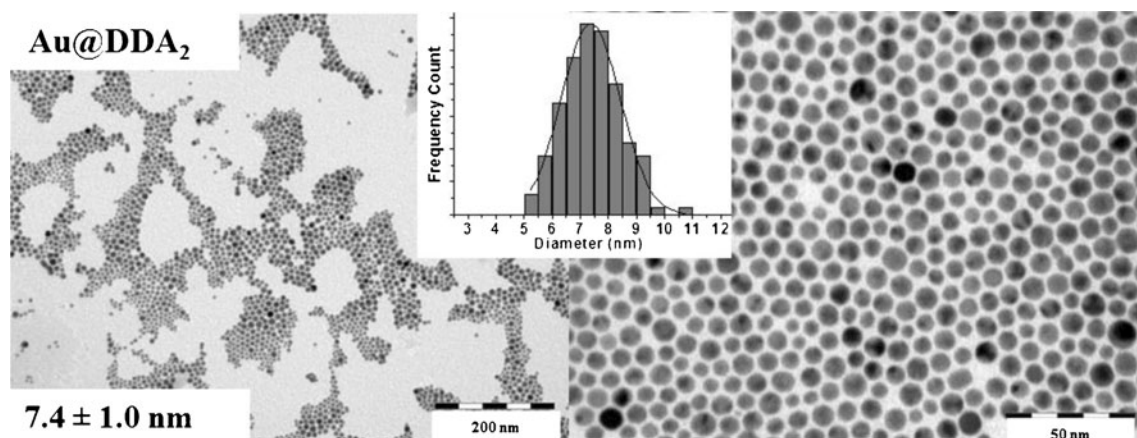


**Fig. 2** Au@DDA<sub>2</sub> obtained from the decomposition of AuCl(THT) with DDA in THF in CO overnight at 70 °C (see Table S1)

the presence of 2.63 and 1.93 ppm signals confirm the formation of AuCl-(HDA) complex as they correspond to free THT also present in the solution.

NMR characterization for the understanding of the stabilization of AuNPs

As the synthesis and behaviour of AuNPs appear to be very similar in the presence of DDA or HDA, NMR characterizations were done randomly on Au@HDA or Au@DDA.

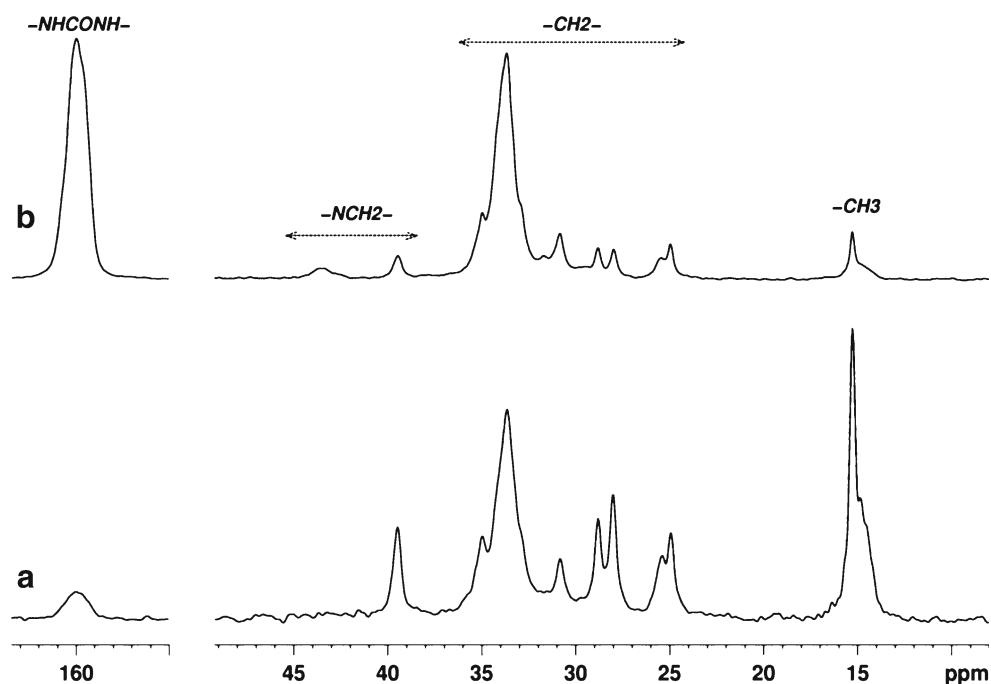
Study of the ligand stabilization of AuNPs after the decomposition of the AuCl(HDA) complex in CO was performed by liquid-state and solid-state NMR experiments. Solid-state NMR allows the characterization of all the ligands involved in the NP stabilization, especially the ones that are poorly mobile close to the NP surface. In liquid-state NMR, only species with enough mobility can be observed. Indeed, relaxation processes strongly broaden the NMR signals of rigid molecules in liquid-state NMR making them difficult or even impossible to detect. However, liquid-state NMR can give important information on the dynamics of the ligands in the NP colloidal solution. Figure 3 shows the solid-state <sup>13</sup>C MAS NMR spectra with direct polarization (DP) or cross polarization (CP) of purified Au@HDA<sub>2</sub> powder with a molar HDA/Au ratio=2. These experiments showed the presence of two species at the surface of the AuNPs. The major compound showed characteristic <sup>13</sup>C NMR signals at 159.9 ppm (carbonyl) and 39.5 ppm (CH<sub>2</sub> bonded to nitrogen) and the signals for the alkyl chain between 15 and 34 ppm. These <sup>13</sup>C chemical shifts are in good agreement with the presence of a carbamide species RNHCONHR resulting from a carbonylation of the HDA. The formation of a carbamido intermediate has already been reported for Pt NPs obtained by the decomposition of Pt(CH<sub>3</sub>)<sub>2</sub>(COD) in CO in the presence of oleic acid and HDA [34]. In the <sup>13</sup>C CPMAS spectrum (Fig. 3b), a second set of signals corresponding to a minor species was observed with notably a signal at 43.6 ppm. This signal at 43.6 ppm is in agreement with a CH<sub>2</sub> group

bonded to a NH<sub>2</sub> function and we assume that it comes from an amine ligand coordinated on the NP surface. The stronger amplification of the 43.6 ppm signal in the CPMAS experiment compared to the DPMAS, indicates that the amine alkyl chain has a more rigid structure than the carbamine alkyl chains, probably having fewer degrees of freedom. Indeed, local mobility reduced the dipolar coupling strength between protons and carbons and therefore the polarization transfer in the CPMAS experiment. From the <sup>13</sup>C DPMAS spectrum, we can deduce that the proportion of unreacted amine is lower than 5 % (the signal at 43.6 ppm was not detected). Furthermore, several signals showed complex line shapes (as one of the terminal methyl and carbonyl groups, ESM S8). This result could indicate the presence of heterogeneous environments for the carbamide which can result from different binding sites at the NP (such as faces, edges or apexes) or different organizations of the ligand. It is also possible that intermediate carbamido complex or urea is present at the AuNP surfaces.

Liquid-state NMR experiments were also performed on purified Au@HDA<sub>2</sub> powder (see “Experimental section”) to monitor the ligand dynamics in the NP colloidal solution. This solution was characterized by <sup>1</sup>H NMR and did not reveal any trace of free HDA, undecomposed AuCl(HDA) complex or THT (Fig. 4a). Signals detected at 1.32 and 0.92 ppm correspond to the methylene or methyl alkyl chain signals of the carbamide and/or of the amine ligands.

Weak additional <sup>1</sup>H resonances at 5.03 and 3.09 ppm were also observed. From 2D <sup>1</sup>H-<sup>1</sup>H COSY and <sup>1</sup>H-<sup>13</sup>C HMBC NMR experiments, these signals were attributed to the NH group (5.03 ppm) and to the methylene signal connected to the nitrogen (δ <sup>1</sup>H 3.09 ppm; δ <sup>13</sup>C 39.8 ppm) of the carbamide species (δ <sup>13</sup>C of carbonyl at 157.2 ppm). They were also connected to the alkyl chain signals at 1.3 and 0.9 ppm by <sup>1</sup>H-<sup>1</sup>H COSY and <sup>1</sup>H-<sup>13</sup>C HMBC experiments. These signals also showed a smaller diffusion coefficient at 0.8 × 10<sup>-9</sup> m<sup>2</sup>·s<sup>-1</sup> than free HDA (1.1 × 10<sup>-9</sup> m<sup>2</sup>·s<sup>-1</sup>) due to a slower diffusion associated with the larger size of the carbamide species.

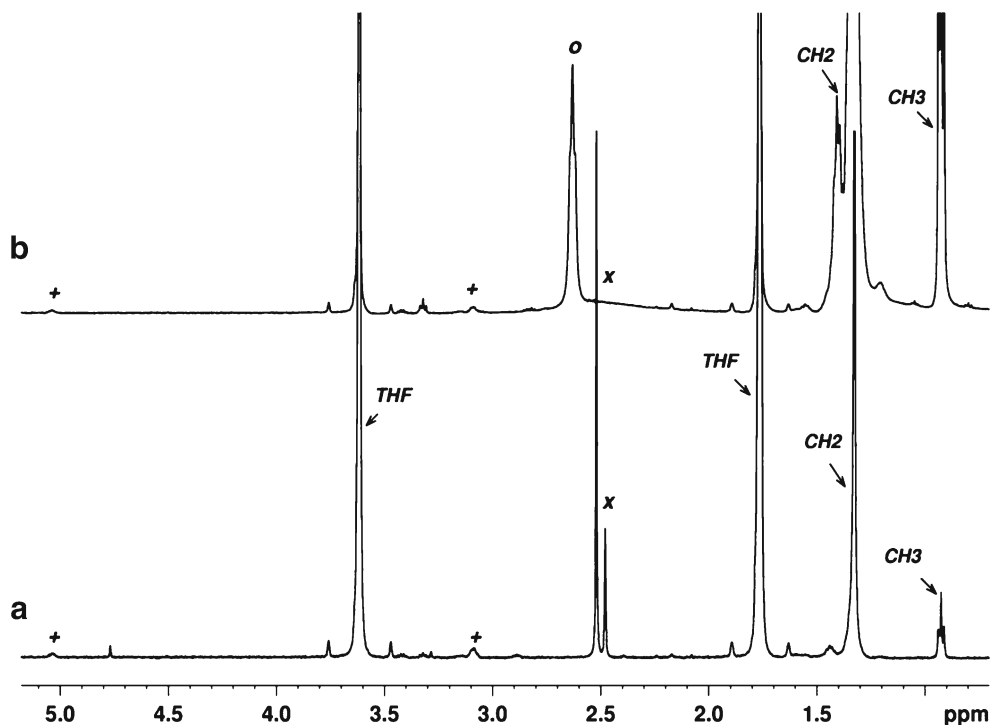
**Fig. 3**  $^{13}\text{C}$  DPMAS (a) and CPMAS (b) NMR of Au@HDA<sub>2</sub> powder



However, this diffusion coefficient is much higher than the one expected for a ligand strongly bound to NP of 7-nm diameter which should be one order of magnitude lower (less than  $1 \times 10^{-10} \text{ m}^2 \cdot \text{s}^{-1}$ ) [35]. These results indicated the presence of a few carbamide species in solution resulting probably from the decooordination from the NP surfaces. The amount of decoordinated carbamide seems however very small. No exchange phenomena between the NP surface and

the solution could be detected for the decoordinated carbamide indicating an irreversible or slow decooordination process compared to the NMR timescales. Furthermore, integration of the methylene (1.32 ppm) and methyl alkyl chain signals (0.91 ppm) compared to that of the NH (5.03 ppm) and  $\alpha\text{-CH}_2$  signals (3.09 ppm) of the carbamide showed an excess of alkyl chain signals (for example the ratio between the  $\alpha\text{-CH}_2$  and the methyl signal is equal to 2/8

**Fig. 4**  $^1\text{H}$  NMR spectra at 25 °C of Au@HDA<sub>2</sub> in THF-d<sub>8</sub> (a) and after addition of two supplementary equivalents of HDA (b). (o: HDA; +: carbamide; x: labile protons (NH<sub>2</sub>, H<sub>2</sub>O,...))



instead of the 2/3 expected for the carbamide). This showed the presence of alkyl chain signals of amine ligands superimposed with one of the free carbamide signals. However, no NMR resonance for the amine extremity, notably the  $\alpha$ -CH<sub>2</sub> at 2.93 ppm of HDA, was observed. Disappearance of NMR signals, related to fast relaxation processes, for nuclei close to the binding site of NPs is a common observation for ligands involved in “intermediate” or slow exchange between the NP surface and the solution [36].

To study the presence of an exchange phenomenon between the NP surface and the solution for HDA, two additional equivalents of HDA were added to the solution of redispersed AuNPs@HDA<sub>2</sub> (Fig. 4b). Sharp signals of HDA were observed after this addition. The diffusion coefficient of HDA in this sample was the same as for free HDA, i.e.  $1.1 \times 10^{-9} \text{ m}^2 \cdot \text{s}^{-1}$ . As the diffusion coefficient and the signal shape of HDA in excess looked very similar to one of the free HDA, a transfer NOE experiment was conducted. This experiment has been reported as a powerful technique for characterizing grafted ligands at the NP surface in rapid exchange with free ligands in the solution even when the amount of the grafted ligand is small compared to the free one [37].

Transferred NOEs were observed for the methylene signal in  $\alpha$ -position of the amine group at 2.63 ppm (ESM S9) but not for the terminal methyl group of HDA at 0.93 ppm which instead showed zero-quantum artifact usually observed for fast tumbling molecules in NOESY experiments with short mixing times [37]. These results indicate that when an excess of HDA is present, the HDA interacts with the AuNPs and is rapidly exchanged between the NP surface and the solution at the NMR timescales. The increase of the exchange rate when the ratio of ligand/NPs increases has already been described and is related to the higher concentration of free ligands [35]. As the transferred NOE was observed on the amine extremity

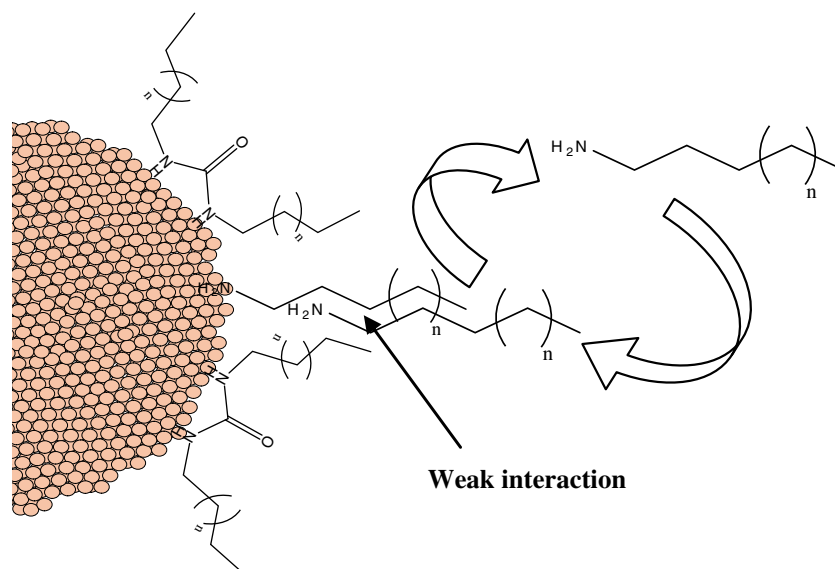
and not on the methyl extremity, this also confirms that HDA interacts with AuNPs through its amine group side (Scheme 2). The fast exchange between the NP surface and the solution observed for the amine indicates the presence of weak binding modes for this ligand.

## Conclusion

In this study, well-controlled syntheses of monodisperse AuNPs of small diameter have been described by the decomposition of AuCl(THT) in a CO atmosphere in the presence of alkylamine (DDA or HDA) only. Purified AuNPs are redispersible and stable in organic solvents for months. NMR characterization has evidenced the formation of a carbamide species resulting from the AuCl(amine) decomposition in CO. Moreover, the solid-state <sup>13</sup>C NMR on purified AuNPs has shown the stabilization of AuNPs by two types of ligands: a majority of carbamide-like species and a few percent of “coordinated” amine. The stabilizing carbamide ligands around the AuNPs are strongly bound to the surface of the AuNPs and do not exchange with free species in solution (in the NMR timescales). Some unreacted amine ligands might still be present and can interact with the AuNPs. The interaction of amine ligands with AuNPs is weaker than that of the carbamide as the amine ligands are able to exchange between the NP surface and the solution.

As a whole, the decomposition of the precursor through carbonylation results in the formation of a better stabilizing ligand than the original amine and explains the long-term stability of the colloidal solutions obtained in this process. The latter is attractive for the surface nanostructuring for chemical sensor applications.

**Scheme 2** Weak interaction of free alkylamine with AuNP surfaces



**Acknowledgment** This work was part of a project financially supported by the Fondation STAE (Sciences et Technologies pour l'Aéronautique et l'Espace) under the acronym "MAISOE" (Microlaboratoires d'Analyses In Situ pour des Observatoires Environnementaux) and ANR (ANR project MOCANANO).

**Open Access** This article is distributed under the terms of the Creative Commons Attribution License which permits any use, distribution, and reproduction in any medium, provided the original author(s) and the source are credited.

## References

1. Dadosh T, Gordin Y, Krahne R, Khivrich I, Mahalu D, Frydman V, Sperling J, Yacobi A, Bar-Joseph I (2005) *Nature* 436:677–680
2. Pradhan S, Sun J, Deng FJ, Chen S (2006) *Adv Mater* 18:3279–3283
3. Somorjai GA, Frei H, Park JY (2009) *J Am Chem Soc* 131:16589–16605
4. Aragay G, Merkoçi A (2012) *Electrochim Acta* 84:49–61
5. Aragay G, Pino F, Merkoçi A (2012) *Chem Rev* 112:5317–5338
6. Jain KK (2007) *Clin Chem* 53:2002–2009
7. Yeh Y-C, Creran B, Rotello V (2012) *Nanoscale* 4:1871–1880
8. Wang B, Anslyn EV (2011) *Chemosensors: Principles, Strategies, and Applications*. John Wiley and Sons, New York, p 163
9. Hossam H (2007) *J Phys D: Appl Phys* 40:7173–7186
10. Zhang X, Guo Q, Cui D (2009) *Sensors* 9:1033–1053
11. Daniel M-C, Astruc D (2004) *Chem Rev* 104:293–346
12. Boissilier E, Astruc D (2009) *Chem Soc Rev* 38:1759–1782
13. Haruta M, Kobayashi T, Sano H, Yamada N (1987) *Chem Lett* 16:405–408
14. Corma A, Garcia H (2008) *Chem Soc Rev* 37:2096–2126
15. Bardhan R, Lal S, Joshi A, Halas NJ (2011) *Acc Chem Res* 44:936–946
16. Schatz GC (2007) *Proc Natl Acad Sci U S A* 104:6885–6892
17. Elghanian R, Storhoff JJ, Mucic RC, Letsinger RL, Mirkin CA (1997) *Science* 277:1078–1081
18. Lian W, Liu S, Yu J, Xing X, Li J, Cui M, Huang J (2012) *Biosens bioelectrocnics* 38:163–169
19. Kumar S, Kwak K, Lee D (2011) *Anal Chem* 9:3244–3247
20. Hezard T, Fajerweg K, Evrard D, Collière V, Behra P, Gros P (2012) *Electrochim Acta* 73:15–22
21. Hezard T, Fajerweg K, Evrard D, Collière V, Behra P, Gros P (2012) *J Electroanal Chem* 664:46–52
22. Li C, Shuford KL, Park QH, Cai W, Li Y, Lee EJ, Cho SO (2007) *Angew Chem Int:Ed* 46:3264–3268
23. Zeng J, Ma Y, Jeong U, Xia Y (2010) *J Mat Chem* 20:2290–2301
24. Schmid G (1992) *Chem Rev* 92:1709–1727
25. Zheng N, Fan J, Stucky GD (2006) *J Am Chem Soc* 128:6550–6551
26. Gomez S, Philippot K, Colliere V, Chaudret B, Senocq F, Lecante P (2000) *Chem Commun* 1945–1946
27. Lu X, Tuan H-Y, Korgel BA, Xia Y (2008) *Chem Eur J* 14:1584–1591
28. Zheng Y, Tao J, Liu H, Zeng J, Yu T, Ma Y, Moran C, Wu L, Zhu Y, Liu J, Xia Y (2011) *Small* 167:2307–2312
29. Lu X, Yavuz MS, Tuan H-Y, Korgel BA, Xia Y (2008) *J Am Chem Soc* 130:8900–8901
30. Philippot K, Chaudret B (2007) In: *Comprehensive Organometallic Chemistry III*, RH Crabtree & MP Mingos, Elsevier, Chapter 12–03: pp71–99
31. Uson R, Laguna A (1986) *Organomet Synth* 3:322–342
32. Axet MR, Philippot K, Chaudret B, Cabié M, Giorgio S, Henry C (2011) *Small* 7:235–241
33. Debouttiere P-J, Coppel Y, Denicourt-Nowicki A, Roucoux A, Chaudret B, Philippot K (2012) *Eur J of Inorg Chem* 8:1229–1236
34. Latour V, Maisonnat A, Coppel Y, Colliere V, Fau P, Chaudret B (2010) *Chem Comm* 46:2683–2685
35. Coppel Y, Spataro G, Pagès C, Chaudret B, Maisonnat A, Kahn ML (2012) *Chem Eur J* 18:5384–5393
36. Hens Z, Martins JC (2013) *Chem Mater* 25:1211–1221
37. Fritzinger B, Moreels I, Lommens P, Koole R, Hens Z, Martins JC (2009) *J Am Chem Soc* 131:3024–3032